Journal of the Geological Society, London, Vol. **166**, 2009, pp. 895–904. doi: 10.1144/0016-76492008-007.

The hydration and alteration of perlite and rhyolite

J. S. DENTON[1], H. TUFFEN[1], J. S. GILBERT[1] & N. ODLING[2]

[1]*Division of Environmental Science, Lancaster Environment Centre, Lancaster University, Lancaster LA1 4YQ, UK*

[2]*School of Geosciences, University of Edinburgh, Grant Institute, King's Buildings, West Mains Road, Edinburgh EH9 3JW, UK*

**Corresponding author (e-mail: j.denton1@lancaster.ac.uk)*

Abstract: The volatile concentrations and thermal characteristics of hydrothermally altered rhyolitic deposits erupted under Icelandic glaciers have been studied by combined differential scanning calorimetry–thermogravimetric analysis–mass spectrometry (DSC–TGA–MS) and X-ray diffraction (XRD). Samples range from pristine obsidians to strongly perlitized and altered fragmental deposits. Four types of samples are determined to have notable differences in total volatile concentrations: obsidians (0.44–3.04 wt%), perlites (2.15–8.15 wt%), obsidian-breccias (8.49–9.41 wt%) and hyaloclastites (3.23–7.78 wt%). DSC–TGA–MS and textural data indicate that the volatile concentration of the perlitic samples increases as the amount of perlitization increases. XRD data show that the volatile-rich samples are rich in the low-temperature zeolite minerals heulandite and mordenite. The temperature at which volatile exsolution occurs is shown to decrease as the volatile concentration increases, reflecting the speciation of water as well as zeolite mineral growth.

Supplementary material: Detailed grain-size fraction analysis data in table and histogram form are available at http://www.geolsoc.org.uk/SUP18366.

Rhyolites, which make up *c*. 10% of the Icelandic crust, are a rare example of silicic volcanic rocks erupted in an oceanic setting (Jónasson 2007). Rhyolitic magma in Iceland is primarily found within or close to central volcanoes that have been active for 0.5–2.5 Ma (Sæmundsson 1978; Gunnarsson *et al*. 1998). In large central volcanoes ($\geqslant$400 km^3) such as Torfajökull they can form up to 20–30% of the exposed rocks and >50% of the central portion (Walker 1963; Gunnarsson *et al*. 1998).

Samples analysed in this study are sourced from two central volcanoes, Torfajökull and Krafla, and reflect a broad range of volcanic lithofacies that include obsidian lavas and variably altered fragmental deposits. We use the term alteration as defined by McPhie *et al*. (1993); that is, the change in mineralogy and texture of a deposit, facilitated by the action of hot or cold aqueous solutions or gases. In many volcanic terranes the processes of diagenetic and hydrothermal alteration are inseparable and involve dissolution, replacement and precipitation of minerals along fluid pathways (Noh & Boles 1989). Volcanic glasses of dacitic and rhyolitic compositions (Noh & Boles 1989; Drysdale 1991) can be altered by hydration to form the industrially important commodity perlite, which is volcanic glass hosting abundant delicate, intersecting and gently curved cracks surrounding cores of intact glass (McPhie *et al*. 1993). Perlitized obsidian is also water rich; studies of hydrogen and oxygen isotopes have shown that this is due to diffusion of meteoric water into the glass and not a water-rich original magma (Ross & Smith 1955; Friedman & Smith 1958, 1960; Marshall 1961; Friedman *et al*. 1966). The meteoric water is reintroduced as molecular water or hydroxyl groups depending on total water content and temperature of hydration (Stolper 1982; Sodeyama *et al*. 1999; Roulia *et al*. 2006). Whether the diffusion of water results in the cracks or crack formation facilitates the diffusion of water is still unresolved (Marshall 1961; Friedman *et al*. 1966).

The further alteration of perlitized obsidian occurs through glass dissolution and smectite crystallization along the perlitic cracks. It manifests itself in a colour change from dark grey to dull brown or green (Noh & Boles 1989). As alteration proceeds glass dissolution and smectite crystallization increase inwards from the cracks, eventually resulting in the central bead of remnant glass being completely dissolved. This alteration pathway is assumed to be appropriate for perlite derived from obsidian of rhyolitic composition; however, the alteration minerals produced are likely to be different (Bagdassarov *et al*. 1999).

Roulia *et al*. (2006) conducted thermogravimetric analysis (TGA) of perlitic samples from Milos, Greece, and other locations, measuring sample mass loss under a controlled heating programme. They found that the proportion of mass lost at low temperatures (0–250 °C; thought to be molecular water) increased when longer isotherms were incorporated into the experimental method. Bagdassarov *et al*. (1999) showed, through TGA and differential thermal analysis (DTA) experiments on perlite glasses, that heat input between 150 and 200 °C was mainly used to vaporize water without driving it from the sample. They described the first peak of a time derivative of the TGA signal as the characteristic temperature of glass dehydration (Bagdassarov *et al*. 1999).

Gaining insights into how perlite forms is valuable because it may provide clues to the environment of eruption, in particular the environment of magma–water interaction (e.g. Davis & McPhie 1996; Tuffen *et al*. 2001). The minerals that have grown in the perlitic fractures may reflect the chemistry of aqueous solutions or gases present post-eruption. Studying the hydration and alteration of volcanic material is important because this is a stage in the soil-forming process.

We present the first study of volatile contents and thermal characteristics of a suite of samples showing varying degrees of alteration from pristine obsidians, through perlites, to highly altered cemented breccias. Other TGA studies on perlite (e.g. Bagdassarov *et al*. 1999; Roulia *et al*. 2006) were not carried out

on samples from such well-constrained geological settings. The samples analysed in this study are sourced from locations where the environment of eruption is relatively well established.

Localities

Samples were analysed from three localities within the Torfajökull central volcano: Bláhnúkur, SE Rauðfossafjöll and Dalakvísl (Fig. 1). Additional samples were analysed from Hrafntinnuhryggur, Krafla central volcano (Fig. 2). A brief overview of the geology of the four localities follows.

Torfajökull central volcano is the largest active silicic centre in Iceland (Tuffen *et al*. 2001), where >80% of outcrops are silicic in composition (Gunnarsson *et al*. 1998). Eruptions during glacial periods have resulted in a series of subglacial and subaqueous silicic formations, with subaerial lavas also present (McGarvie 1984; Tuffen *et al*. 2001).

Bláhnúkur (Fig. 1) formed in a small-volume effusive sub-

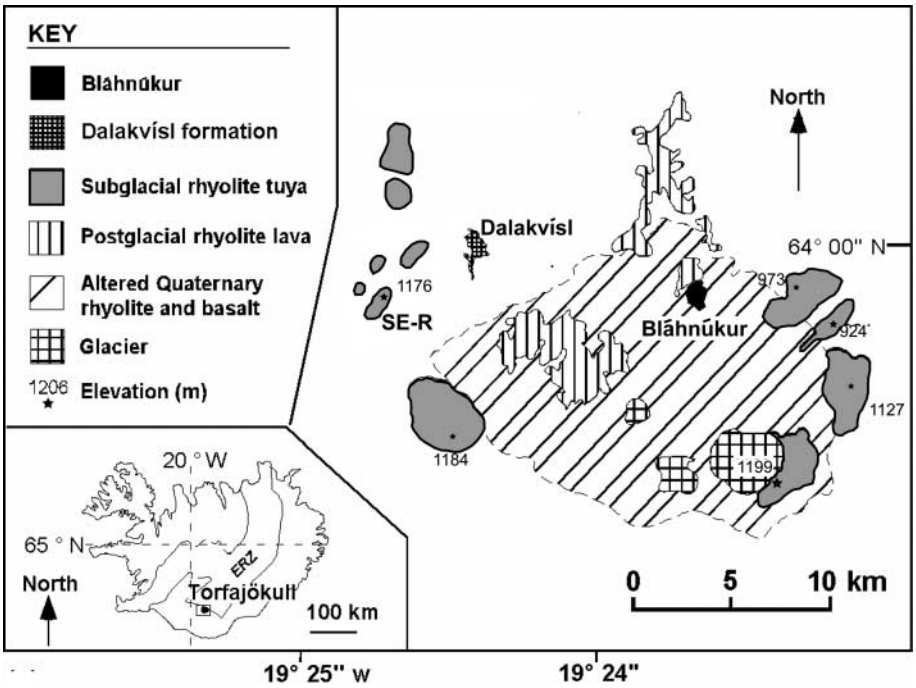

Fig. 1. Map showing the three localities, Bláhnúkur, SE Rauðfossafjöll (SE-R) and the Dalakvísl formation, within the Torfajökull central volcano (modified from Tuffen 2001). ERZ, Eastern Rift Zone.

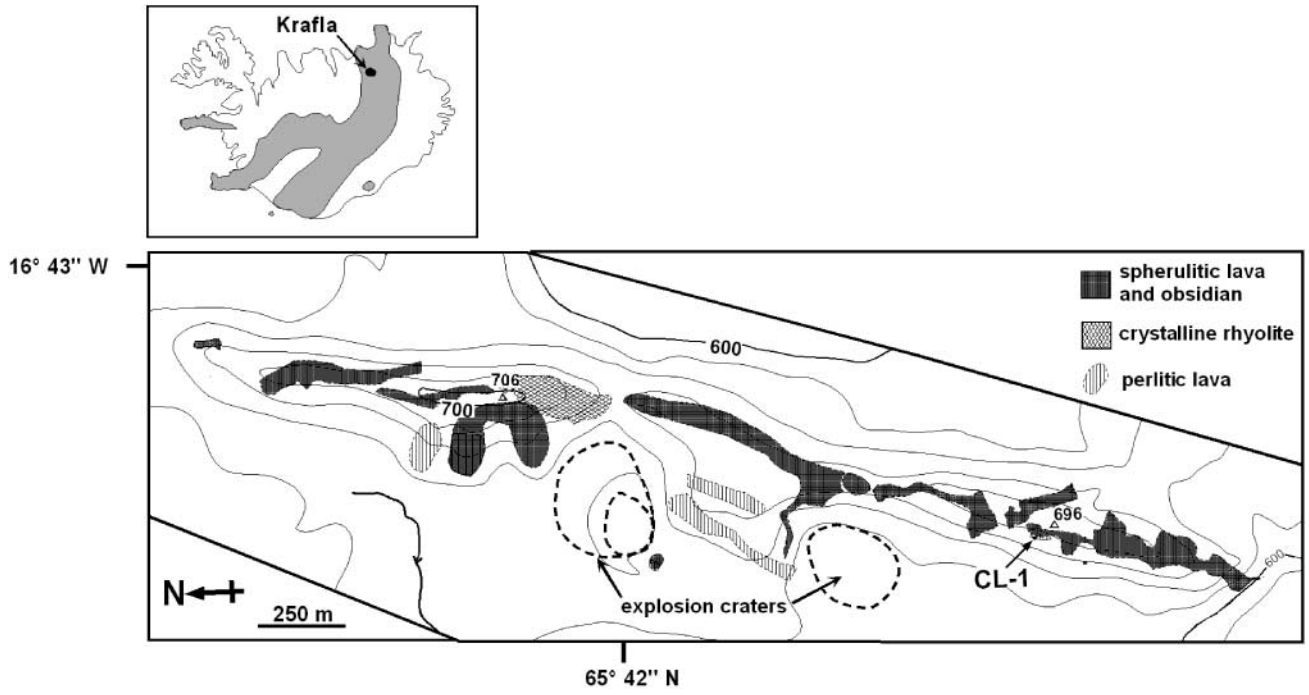

Fig. 2. Map showing the geology of Hrafntinnuhryggur within the Krafla central volcano (modified from Tuffen & Castro 2009). CL-1 marks the location of the Krafla sample analysed in this study.

glacial eruption during the last glacial period (115–11 ka ago). Deposits are dominated by irregular- to cylindrical-shaped obsidian (sometimes perlitized) and microcrystalline rhyolite lobes in a pale grey perlitized hyaloclastite breccia. Other facies include matrix- and clast-supported breccias and columnar-jointed lava flows (Tuffen *et al*. 2001).

Rauðfossafjöll was formed in a larger-volume, more explosive, subglacial eruption than Bláhnúkur and occurred at *c*. 60 ka. The best exposure is on the SE tuya (a steep-sided subglacially erupted volcano with a flat top of subaerially erupted lava (Mathews 1947); Fig. 1; SE-R) and it is from here that the samples analysed were sourced (Tuffen *et al*. 2002). The lower portion of the tuya is dominated by fine-grained ash facies and the summit is capped by subaerial rhyolite lava flows (Tuffen *et al*. 2002).

The Dalakvísl rhyolite formation occurs NE of Rauðfossafjöll (Fig. 1); it is geochemically similar to the tuyas and thus is thought to be contemporaneous at *c*. 60 ka (Tuffen *et al*. 2008). The formation includes both explosive and effusive deposits including breccias and lavas. The dominant lithology is a massive obsidian and pumice breccia. Other facies include a highly vesicular pyroclastic deposit, local well-bedded ash deposits, obsidian (sometimes perlitized) and microcrystalline rhyolite lavas and lava lobes, as well as peperitic lavas (Tuffen *et al*. 2008).

Krafla (Fig. 2 inset) is a central volcano with a basaltic fissure swarm of 100 km length. At *c*. 24 ka a $<0.05\ km^3$ rhyolitic eruption through thin ice formed Hrafntinnuhryggur (Obsidian Ridge, CL-1; Fig. 2; Tuffen & Castro 2009). Lithofacies include numerous small-volume perlitic and spherulitic lava bodies set in quench hyaloclastites, obsidian scree and strongly altered, perlitic, columnar-jointed obsidian. Locally quench-fragmented, perlitic lavas grade outwards into indurated breccia cemented by alteration minerals.

Samples analysed

A brief geological description and summary of the samples analysed is given in Table 1. Field observations from the lithofacies have been given by Tuffen *et al*. (2001) (Bláhnúkur), Tuffen *et al*. (2002) (Rauðfossafjöll), Tuffen *et al*. (2008) (Dalakvísl) and Tuffen & Castro (2009) (Hrafntinnuhryggur).

Methods

Petrographic observations

Microtextural observations were performed using a petrological microscope. The degree of perlitization was estimated using the relative proportion of arcuate cracks and surrounding darker hydrated glass to unhydrated, pale cream glass.

Particle size

The grain-size distributions of unconsolidated samples were determined by sieving. The percentage of obsidian in each size fraction was also estimated by eye.

Volatile contents

Volatile contents and thermal characteristics of samples were analysed by differential scanning calorimetry–thermogravimetric analysis–mass spectrometry (DSC–TGA–MS) using a TA Instruments SDT Q600 simultaneous DSC–TGA instrument coupled to an HPR-20 QIC Gas Analysis System mass spectrometer at Lancaster University. The DSC–TGA technique measures the weight loss and thermal characteristics of a sample while it is subject to a controlled heating programme. The addition of the mass spectrometer allows the identification of the exsolved gases. In the current set-up it is not routinely possible to resolve H_2O from other volatiles such as Cl and F when volatile contents are low. Nevertheless, the dominance of H_2O over other volatiles (e.g. Cl and F) in volatile-rich samples is demonstrated in greater counts per second by several orders of magnitude. During analysis the sample was purged by oxygen-free nitrogen with better than 99.999% purity at a flux of 50 ml min^{-1}.

Each sample was crushed and sieved. The 125–500 μm size fraction was washed with acetone and then oven-dried at 110 °C for *c*. 1 h (Newman *et al*. 1986). After drying, the sample was transferred to a desiccator to minimize atmospheric water adsorption before analysis. Approximately 30 mg of the sample was placed in a tared platinum cup on the DSC–TGA sample beam and heated at 5 °C min^{-1} from ambient temperature to 1250 °C, and then held at this temperature for 2 h. The sample was then cooled to ambient temperature and the heating was repeated. This allowed artefacts inherent to the instrumentation to be removed from the results. Performing a second heating, which recorded no volatile loss, for each sample also confirmed that the heating method employed successfully drove off all the volatiles. Total volatile loss (i.e. total volatile content) was calculated by subtracting the second heating weight loss from the first heating weight loss. The temperatures of minimum heat flow and of maximum differential mass loss (dTG) were determined for each sample (Fig. 3). The maximum MS water signal was also determined for each sample, based on the assumption that water was the dominant dissolved volatile species (Fig. 3). This method was repeated for at least one duplicate of each sample.

We also investigated the effect of grain size on volatile content in altered fragmental deposits. This was undertaken first for sample D85a from Dalakvísl (Table 1). The sample was sieved into six size fractions (>500, 355–500, 180–355, 106–180, 38–106 and <38 μm). Each size fraction was analysed by DSC–TGA–MS. Samples from Bláhnúkur (B120a) and SE Rauðfossafjöll (D-0016) were also analysed but using only two size fractions from each. To avoid adding unnecessary variables to the experiments the >500 μm fraction for all samples was crushed to 125–500 μm as this was the standard size range used for volatile content analyses in this study and by Newman *et al*. (1986).

Secondary mineral growth

X-ray diffraction (XRD) analysis was carried out on six samples (Table 5) at the University of Edinburgh, to investigate whether contrasting alteration minerals and concentrations are present for (1) perlites and unconsolidated samples and (2) grey and green units.

Samples were ground to *c*. 50 μm in an orbital mill; *c*. 2 g of this material was loaded into a micronizing mill along with 10 cm^3 of de-ionized distilled water and the mixture was ground for 12 min. A few drops of the resulting suspension were then placed onto a glass plate and dried in air at 60 °C. This preparation method, although producing well-defined diffraction peaks, inevitably introduces an unknown but significant degree of preferred orientation into the samples for those minerals that have platy or rod-like habits, thus increasing the reflections with $l \neq 0$. The effects of preferred orientation can be compensated

Table 1. *Geological and selected petrological descriptions of the samples analysed in this study*

Sample	Location and grid reference	Geological description	Lithofacies description	Degree of perlitization in thin section (%)	Petrological description of perlitized samples
GD-2	SE Rauð [7862 9596]	Perlitic obsidian from slowly cooled dome thoroughly fluxed with glacial meltwater	Lava F [1]	25	Intact pale cream glass, planar and curviplanar fractures connected by arcuate fractures generating beads *c*. 0.5 mm in diameter
D-0016	SE Rauð [7840 9430]	Green ash	Base of lava D [1]	0	
PLAT-18	SE Rauð 7851 9533	Grey perlitic lava	Lava D [1]	20	Intact yellow glass, planar and curviplanar fractures, occasionally linked by arcuate fractures generating incomplete beads
TCOG-1 and TCOG-2	SE Rauð [7877 9618]	Breccia	Rhyolitic ash [1], sample from a coarse horizon	0	
TCO-1	SE Rauð [7705 9455]	Obsidian from subaerial lava flow	Lava B [1]	0	
TCO-7	SE Rauð [7790 9565]	Obsidian with angular tuffsite veins (West Wall)	Lava B [1]	0	
Summary	*SE Rauð*	*2 hyaloclastites, 2 perlites and 2 non-perlitized obsidians*			
D-001	Dalak [8150 9910]	Ash/pumice hyaloclastite from margin of columnar-jointed lava lobes	Hyaloclastite from lava 2 margin [2]	0	
D-003	Dalak [8150 9910]	Ash, massive poorly sorted obsidian pumice breccia	Breccia 1 [2]	0	
D-0010	Dalak [8156 9958]	Perlitic, indurated ash–pumiceous obsidian breccia	Breccia 1 [2]	90	Intact highly altered brown glass, contains arcuate fractures and pale cream glass beads (*c*. 0.5 mm in diameter)
D47-7	Dalak [8193 9975]	Vesicular breccia	Breccia 2 (2 m from stringer) [2]	0	
D85a	Dalak [8213 9930]	Green poorly consolidated, crudely bedded, well-sorted ash	Breccia 3 [2], sample from an ash horizon	0	
Summary	*Dalak*	*4 hyaloclastites and 1 perlite*			
B25a	Bláhnúkur [9491 9630]	Green perlitic obsidian from ash matrix-supported polymict breccia	Breccia D [3]	30	Fragmental with pale cream glass clasts (up to 1 cm in size) in a pale brown matrix. Planar and curviplanar fractures sometimes bridged by shorter planar cracks. Arcuate fractures form beads *c*. 0.1–0.2 mm in diameter. Many beads have concentric circles of arcuate fractures
B45a	Bláhnúkur [9428 9644]	Interior vesicular portion of lava lobe	Lava lobe-breccia A [3]	0	
B45b	Bláhnúkur [9428 9644]	Sheared obsidian margin of lava lobe	Lava lobe-breccia A [3]	0	
B194a	Bláhnúkur [9453 9580]	Matrix-supported vesicular obsidian breccia from the base of columnar-jointed lava	Columnar-jointed lava [3]	0	
B120a	Bláhnúkur [9406 9614]	Pumiceous ash breccia at margin of lava lobe	Lava lobe-breccia A [3]	0	
B120b	Bláhnúkur [9406 9614]	Perlitic obsidian lobe margin with extensive alteration	Lava lobe-breccia A [3]	20	Intact pale cream glass, irregular network of planar and curviplanar fractures, occasionally linked by arcuate fractures generating beads *c*. 0.5 mm in diameter
Summary	*Bláhnúkur*	*1 quenched hyaloclastite, 2 perlites, 2 non-perlitized obsidians and 1 non-perlitized obsidian-breccia*			
Krafla perlite	Krafla [6955 8665]	Quenched fractured margin of a lava flow or dome	Lava flows and domes [4]	50	Intact yellow glass, planar fractures joined by arcuate fractures forming beads *c*. 0.2 mm in diameter
Krafla bead	Krafla [6955 8665]	Obsidian bead within the grey friable perlite	Lava flows and domes [4]	0	
Summary	*Krafla*	*1 perlite and 1 non-perlitized obsidian*			

SE Rauð, SE Rauðfossafjöll; Dalak, Dalakvísl. References: [1] Tuffen *et al.* (2002); [2] Tuffen *et al.* (2008); [3] Tuffen *et al.* (2001); [4] Tuffen & Castro (2009).

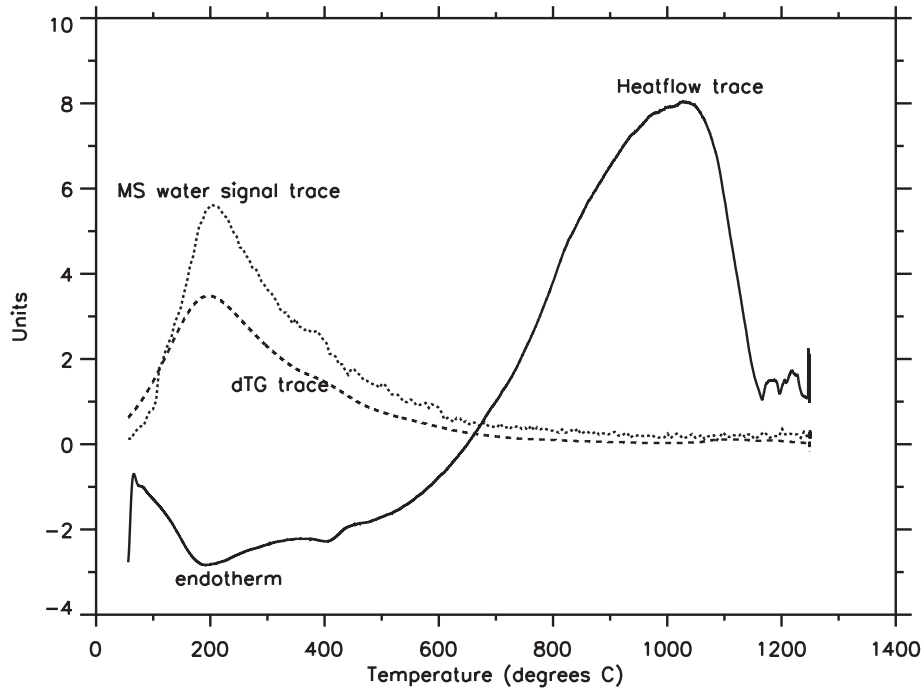

Fig. 3. Temperature (°C) of minimum heat flow (reflecting the endotherm of degassing) (continuous line), of peak differential mass loss (rate of mass loss; dTG) (mg min^{-1}) (dashed line) and of the peak MS water signal (counts per second) (dotted line) for a typical sample of this study. So that the data plot on the same graph the dTG data have been multiplied by 10^2 and the MS water signal by 10^9. The temperature of the two peaks and the endotherm were recorded as the temperature of degassing.

for by the Rietveld analysis package. The powder diffraction data were recorded on the Bruker D8 Advance Diffractometer at the School of Geosciences, University of Edinburgh. The amounts of phases present were determined by the Rietveld analysis package Topas 3, in which the observed diffraction pattern is fitted against a synthetic pattern derived from a sum of patterns calculated for each phase present in the sample. The difference between the observed pattern and the synthetic pattern is minimized by an interactive refinement–optimization procedure to derive an estimate of the amounts of the phases present.

Results

Petrography

Photomicrographs of perlitic samples are shown in Figure 4. These samples are described briefly in Table 1. The arcuate (perlitic) fractures form complete and incomplete beads. The perlitic fractures form from the more prominent planar or curviplanar fractures that form a boundary around areas of perlitized glass. Planar cracks are wider than the arcuate fractures. Alteration minerals form within planar, curviplanar and arcuate fractures (e.g. the dark colouring of the fractures in Fig. 4b).

Particle size

The grain-size distributions of the hyaloclastites (see Supplementary Publication) contain information on the fragmentation and transport mechanisms involved in the formation of the deposit. D-0016 and D85a are skewed to the finer fractions, consistent with a quench-generated hyaloclastite (Heiken 1972; Heiken & Wohletz 1985). TCOG-2, D-003, D47-7 and B120a are all dominated by coarse particle sizes, indicating explosive generation (Heiken 1972; Heiken & Wohletz 1985). A number of these particles are vesicular (Tuffen 2001; Tuffen *et al*. 2001, 2002, 2008). D-001 has a dominant size range of 0.5–1.0 mm but is bimodal. It is interpreted to have been formed from quench fragmentation of a subglacial lava lobe (Tuffen *et al*. 2008). This explains the high proportion of obsidian.

Volatile contents

Because the CO_2 content of Torfajökull obsidians is negligible (Tuffen *et al*. 2008) and S concentrations are <100 ppm (Tuffen, unpubl. data, Bláhnúkur obsidians), the volatile species present are predominantly H_2O (0.1–0.2 wt%) and halogens ($\leqslant$0.5 wt%) (Tuffen, unpub. data; Table 2). Halogens are unlikely to be mobilized in the hydration process, and thus are likely to contribute no more than 0.4 wt% to the total volatile concentrations in all samples. These measurements are consistent with our mass spectrometer data (CO_2 and SO_2 levels of counts per second of 10^{-11} to 10^{-13} compared with *c*. 10^{-9} for water and no evidence of Na release). Consequently, water is by far the dominant volatile species in the altered samples. Therefore the total volatile content of samples refers to water plus other minor species. The contribution to mass loss of these minor species decreases as the amount of hydration or alteration increases.

Table 3 and Figure 5 present the total volatile contents (wt%) of all the samples analysed in this study. Totals range from 0.52 wt% for obsidians to 9.41 wt% for a green cemented breccia. The total volatile content of the pristine, subaerial obsidian sample TCO-7 measured in this study by TGA (0.52–0.60 wt%) is closely comparable with the sum of independent measurements of H_2O, Cl and F conducted on this sample using Fourier transform IR spectrometry and electron probe analysis (Tuffen, unpubl. data). As total [Cl + F] is typically less than 0.4 wt% in the Torfajökull obsidians analysed, the total volatile contents of all other samples are therefore dominated by H_2O. The subaerial obsidian lavas from SE Rauðfossafjöll and Krafla contain 0.52–0.60 wt% and 0.44–0.65 wt% volatiles, respectively. The subglacially erupted obsidian from Bláhnúkur is notably more volatile rich and the total volatile concentrations are more variable, ranging from 1.05 to 3.04 wt%.

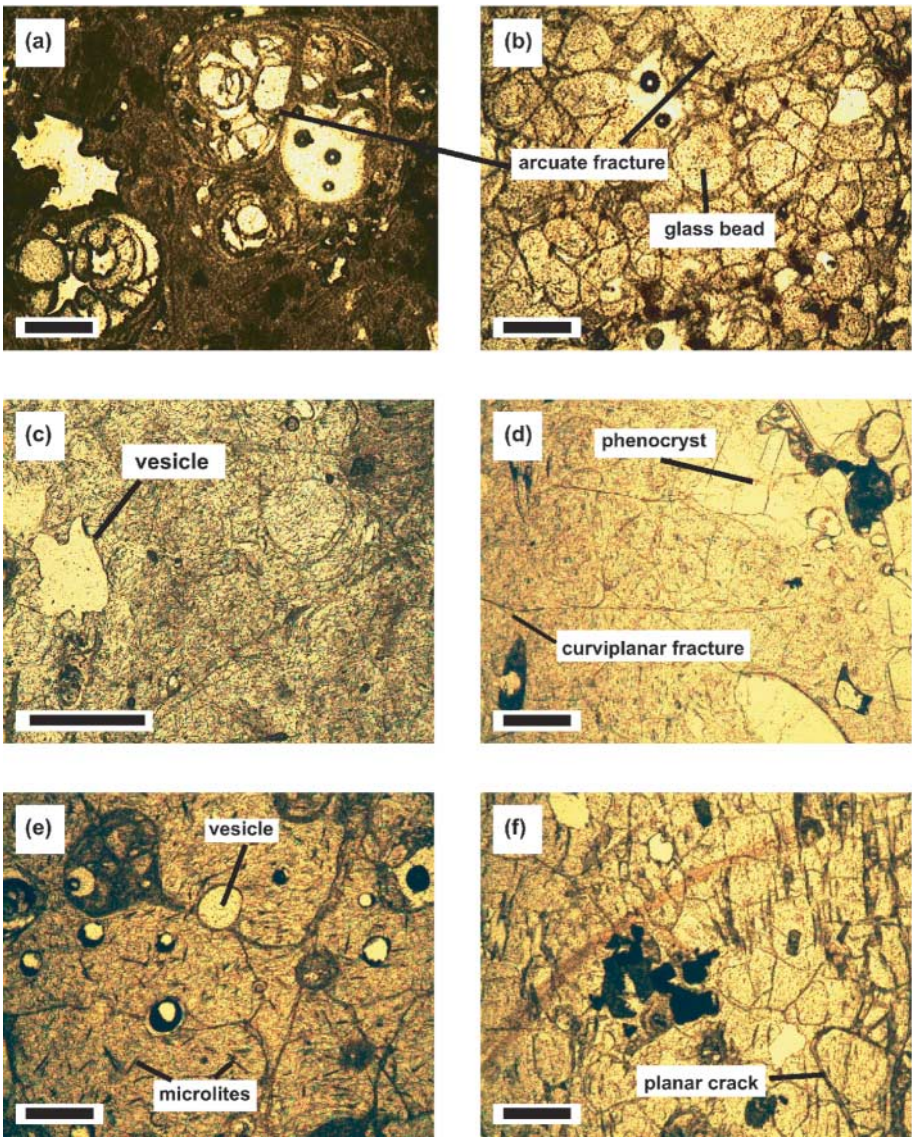

Fig. 4. Photomicrographs of the perlite samples in order of decreasing degree of perlitization; (**a**) D-0010 (SE Rauðfossafjöll), 90% perlitized (the dark areas are more altered, presumed to be perlitized material, and the pale areas are less altered glass); (**b**) CL-1 (Krafla), 50% perlitized; (**c**) B25a (Bláhnúkur), 30% perlitized; (**d**) GD-2 (SE Rauðfossafjöll), 25% perlitized; (**e**) PLAT-18 (SE Rauðfossafjöll) 20% perlitized; (**f**) B120b (Bláhnúkur) 20% perlitized. Scale bars represent 0.5 mm.

Table 2. *Electron probe major element geochemistry (wt%) of three Torfajökull obsidians*

Element	B1 (SD)	D1 (SD)	D2 (SD)
SiO_2	72.319 (0.667)	75.476 (0.153)	75.360 (0.224)
TiO_2	0.206 (0.021)	0.330 (0.017)	0.327 (0.015)
Al_2O_3	13.674 (0.556)	13.015 (0.052)	12.938 (0.075)
MgO	0.087 (0.029)	0.154 (0.010)	0.154 (0.007)
CaO	0.459 (0.121)	0.544 (0.013)	0.540 (0.013)
MnO	0.069 (0.011)	0.118 (0.008)	0.120 (0.008)
FeO	2.388 (0.280)	2.380 (0.040)	2.377 (0.032)
Na_2O	2.958 (0.745)	1.855 (0.092)	1.607 (0.103)
K_2O	4.788 (0.296)	4.052 (0.036)	4.045 (0.042)
P_2O_5	0.016 (0.009)	0.018 (0.008)	0.020 (0.010)
F	0.205 (0.035)	0.160 (0.033)	0.160 (0.036)
Cl	0.197 (0.038)	0.098 (0.018)	0.091 (0.020)
Total	97.365 (0.718)	98.201 (0.158)	97.739 (0.297)

B1 is from Bláhnúkur lava lobe-breccia A (Tuffen *et al.* 2001). D1 is a low vesicular obsidian core and D2 is a transitional obsidian, both from the obsidian stringer facies (breccia 2) at Dalakvísl (Tuffen *et al.* 2002). Data from Tuffen (2001). All data are in wt% to three decimal places. SD, standard deviation.

The total volatile contents of the hyaloclastites vary greatly between localities. The SE Rauðfossafjöll hyaloclastites contain between 6.12 and 7.31 wt% volatiles. Those from Bláhnúkur contain 4.91–5.19 wt% and those from Dalakvísl 3.23–8.15 wt%. This wide range is characterized by a colour change between the grey volatile-poor (3–4 wt%) and the green volatile-rich (7–8 wt%) samples. The green obsidian-breccia from Bláhnúkur has a total volatile content between 8.49 and 9.41 wt%.

The variable total volatile content of SE Rauðfossafjöll perlites corresponds to the degree of perlitization. The GD-2 sample is 25% perlitized and is slightly more volatile rich (3.60–3.81 wt%) than PLAT-18 (20% perlitized and 2.15–2.58 wt%). PLAT-18 Bag was analysed using the method of Bagdassarov *et al*. (1999) and yielded a total volatile content of only 0.39 wt%. This suggests that Bagdassarov *et al*.'s (1999) method using our TGA–MS system failed to remove all the volatiles from the sample because of the absence of vacuum conditions. The Krafla perlite contains 2.47–2.85 wt% total volatiles; thus it is comparable with PLAT-18 but is more strongly perlitized. The Bláhnúkur perlites range from 2.15 to 7.06 wt%, with the perlite that is

Table 3. *Total volatile contents, and temperatures of the minimum heat flow (endotherm of degassing), peak differential mass loss (dTG) and MS water signal*

Sample	Total volatile loss (wt%)	Temperature of endotherm peak (°C)		Temperature of dTG peak (°C)		Temperature of water peak (°C)	
GD-2	3.81	495		314		321	
GD-2 repeat	3.60	512		306		306	
D-0016	6.87	201		271		258	
D-0016 repeat	6.12	200		280		282	
PLAT-18	2.58	635		–		–	
PLAT-18 repeat	2.15	–		–		–	
PLAT-18 repeat 2	2.28	–		–		–	
PLAT-18 Bag.	0.39	–		–		–	
TCOG-1	7.31	206		278		282	
TCOG-1 repeat	7.24	220		280		285	
TCO-1	0.54	729		–		144	
TCO-1 repeat	0.54	663		–		903	
TCO-7	0.60	653		200		109	
TCO-7 repeat	0.52	676		202		816	
D-001	3.48	400		366		384	
D-001 repeat	3.23	437		360		378	
D-003	3.64	418		193		400	
D-003 repeat	3.26	475		396		392	
D-0010	8.04	149		145		98	
D-0010 repeat	8.15	148		143		148	
D47-7	3.82	466		354		370	
D47-7 repeat	3.41	433		348		333	
D-85a	6.95	206		215		213	
D-85a repeat	7.78	198		207		210	
B25a	5.87	541		203		–	
B25a repeat	7.06	692		220		–	
B45a	1.52	553		–		725	
B45a repeat	1.05	514		–		615	
B45a repeat 2	3.04	696		195		–	
B45b	0.96	560		877		–	
B45b repeat	1.61	565		844		–	
B45b repeat 2	1.14	549		855		728	
B45b repeat 3	0.97	655		838		614	
B194a	8.86	105		135		–	
B194a repeat	9.10	105		130		–	
B194a repeat 2	9.41	134		131		–	
B194a repeat 3	8.49	115		138		144	
B120a	4.91	–		–		–	
B120a repeat	5.19	441		299			
B120b	2.15	540		395		402	
Krafla perlite (CL-1)	2.47	608		397		411	
Krafla perlite (CL-1) repeat	2.85	569		300		386	
Krafla bead	0.65	589		556		623	
Krafla bead repeat	0.44	654				286	
Sample type		*T* (°C)	Range	*T* (°C)	Range	*T* (°C)	Range
Hyaloclastite		198–475	277	193–396	203	210–400	190
Perlite		148–692	544	143–397	254	98–411	313
Obsidian		589–729	140	195–556	361	109–903	794
Obsidian-breccia		105–134	29	130–138	8	144	0

Summary temperature ranges for each lithofacies type are also presented. –, no distinct peak in the trace; instead, several smaller peaks were present.

most volatile rich (B25a) being the most perlitized (30%) in thin section and green in colour. The grey Dalakvísl perlite (D-0010) is the most perlitized of all samples studied and is the most volatile rich (90% perlitized with 8.04–8.15 wt% volatiles).

DSC–TGA

Table 3 presents the endotherm, differential mass loss and MS water signal peak temperatures for the samples analysed (Fig. 3). There is considerable variation in the peak temperatures. The range in peak temperatures is generally greater for the pristine obsidians than the other samples (Table 3). We think this may reflect the different coordination of water within the silicate structure as well as the increased contribution of minor species (e.g. Cl and F). Figure 6 shows how the temperature of minimum heat flow, peak differential mass loss and MS water signals vary with total volatile content. The scatter is generally greater when volatile contents are low. Samples with higher total volatile concentrations generally degas at lower temperatures.

Grain-size effect on volatile content

Table 4 shows that the fine grain-size fraction of the Bláhnúkur and SE Rauðfossafjöll hyaloclastites contains more volatiles than the coarse fraction. The Dalakvísl hyaloclastite shows little variation in total volatile content between fractions.

Table 4. *Total volatile contents of three ash fractions taken from Bláhnúkur (B120a); SE Rau*ðfossafjöll (D-0016); and Dalakvísl (D85a)

Grain size (μm)	B120a	D-0016	D85a
>500	4.11	5.94	6.86
355–500	×	×	6.42
180–355	×	×	6.64
106–180	×	×	7.11
38–106	6.49	6.96	7.13
<38	×	×	6.94

×, no analysis.

XRD analysis

Table 5 presents XRD data for six samples analysed. The alteration minerals detected are the zeolites mordenite ($(Ca,K_2,N_2)Al_2Si_{10}O_{24}.7H_2O$) and heulandite ($CaAl_2Si_7O_{18}.6H_2O$). The proportion of both minerals in the green altered samples is greater than or equal to that in the grey samples. The exception, heulandite in the perlites, is approximately constant within analytical error. The hyaloclastites contain no heulandite. Heulandite is softer than mordenite and therefore is thought to have been either weathered and removed from the fragmental samples or not to have formed at all. B194a contains the greatest proportion of both mordenite and heulandite. B194a is a hard, well-consolidated breccia from the eastern flank of Bláhnúkur that has been altered to a green colour. Both mordenite and heulandite contain *c*. 14 wt% H_2O (Deer *et al*. 1963). The water content held in the zeolite minerals (based on 14% H_2O, and the crystalline content of the rock) is compared with the total volatile content of the sample (determined by DSC–TGA–MS) (Table 5).

Discussion

The concentration of magmatic volatiles in non-hydrated glasses is variable and depends on the eruption environment. Subglacially erupted obsidian from Bláhnúkur (Fig. 5) is notably richer in volatiles than subaerially erupted obsidian from SE Rauðfossafjöll and Krafla. This reflects the partial degassing that occurs under elevated pressures during subglacial eruptions. Figure 5 and Tables 1 and 3 demonstrate that as obsidian becomes more perlitized the total volatile content increases. D-0010 is considered to be the most perlitized obsidian (90%) and is the most volatile rich (8.04–8.15 wt%). GD-2 is more perlitized than PLAT-18 (25% and 20%, respectively) and contains more dissolved volatiles (3.60–3.81 wt% compared with 2.15–2.58 wt%). GD-2 and PLAT-18 are from the same locality, confirming that perlitization is driven by water ingress rather than a difference in external factors such as eruption type or climate. Conversely, the Krafla perlite (CL-1) has similar total volatile contents to PLAT-18 despite being more perlitized. This is because the initial total volatile content of the Krafla obsidian was much lower than that of the subglacially erupted PLAT-18 (Tuffen *et al*. 2002; Tuffen & Castro 2009).

One of the unaltered beads from CL-1 was isolated for volatile analysis and found to not be hydrated (0.44–0.65 wt% total volatiles; Fig. 5, Krafla obsidian). This shows that the hydrating water in perlites is concentrated in the altered zones directly adjacent to cracks. This corroborates the results of Saisuttichai &

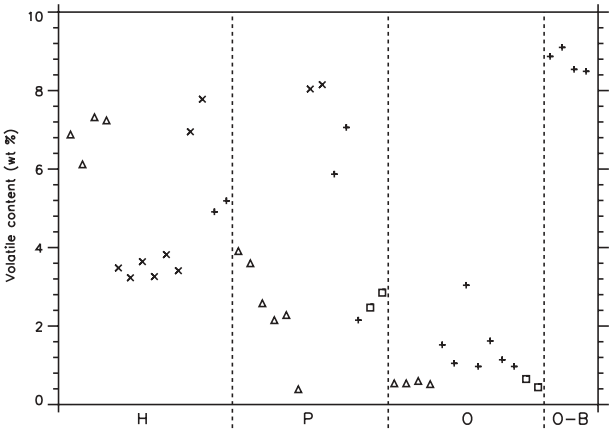

Fig. 5. Total volatile content (wt%) for the samples analysed in this study. H, hyaloclastite; P, perlite; O, obsidian; O-B, obsidian-breccia. Triangles, samples from SE Rauðfossafjöll; ×, samples from Dalakvísl; +, samples from Bláhnúkur; squares, samples from Krafla.

Table 5. *XRD data for selected samples*

Mineral	B25a (green perlite)		PLAT-18 (grey perlite)		D85a (green hyaloclastite)		D-001 (grey hyaloclastite)		B194a (green obsidian-breccia)		B120a (grey breccia)	
	30% perlitized		20% perlitized		non-perlitized		non-perlitized		non-perlitized		non-perlitized	
	Wt%	Error	Wt%	Error	Wt%	Error	Wt%	Error	Wt%	Error	Wt%	Error
Quartz	6.00	0.48	4.89	0.38	20.32	0.86	7.46	0.43	5.37	0.33	20.41	0.58
Mordenite	7.06	1.10	3.30	0.66	11.57	1.40	4.30	1.10	21.76	0.85	13.23	1.0
Heulandite	4.74	1.00	6.02	0.82	0.00	1.20	0.00	0.80	28.44	1.00	0.00	1.0
Albite	12.75	1.50	30.71	1.50	18.54	1.90	24.26	1.30	7.19	1.10	19.12	1.7
Anorthite	69.44	2.10	55.04	1.60	49.45	2.70	63.84	1.70	37.27	1.50	47.23	2.2
Crystalline proportion	10		15		–		–		10		–	
% H_2O based on crystalline proportion of M and H	0.17		0.20		–		–		0.70		–	
Total volatile content	5.87–7.06		2.15–2.58		6.95–7.78		3.23–3.48		8.49–9.41		4.91–5.19	

M and H are mordenite and heulandite, respectively. The percentage water is calculated by totalling the mordenite and heulandite proportions and calculating 14% of the total.

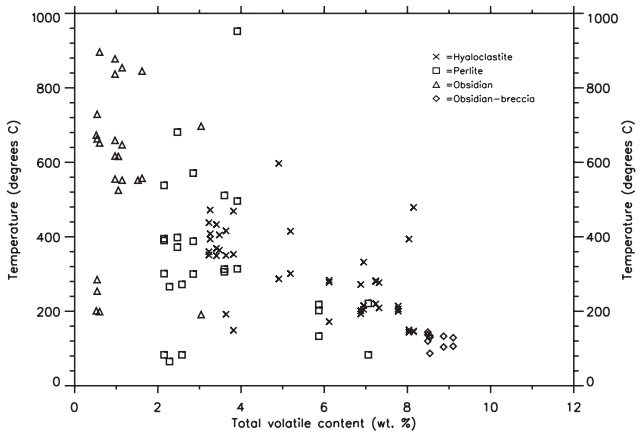

Fig. 6. Temperatures of the minimum heat flow (endotherm of degassing), the derivative mass loss peak (mg min^{-1}) and the peak MS water signal for samples as a function of total volatile content. Together these represent the temperatures of peak volatile exsolution.

Manning (2007), who published bulk electron microprobe data from Thai perlitic rhyolites, with total volatile contents of 0–3.1 wt% estimated from loss on ignition. Therefore the 'bulk' measurement of perlite total volatile contents (e.g. Krafla perlite, 2.47–2.85 wt%) depends on the proportion of unaltered glass (beads) relative to the sample volume analysed.

The total volatile contents of the hyaloclastites vary between localities (Fig. 5). Possible reasons include different eruption types (explosive at SE Rauðfossafjöll, effusive at Bláhnúkur and mixed at Dalakísl (Tuffen *et al*. 2001, 2002, 2008)). The factors likely to control the extent of hydration include the time scale and temperature of magma–water interaction during initial fragmentation and deposition, the rate of cooling and availability of meltwater after deposition (e.g. Drysdale 1991), the grain size of deposits (discussed below), and subsequent reheating (e.g. by lava bodies intruding water-saturated hyaloclastites). Table 4 confirms that the extent of hyaloclastite alteration could also be grain size dependent. The finer grain-size fraction contains more volatiles than the coarser fraction at Bláhnúkur (B120a) and SE Rauðfossafjöll (D-0016). The Dalakvísl hyaloclastite (D85a) shows little variation in total volatile contents between fractions, suggesting equal hydration of all grain sizes. D85a is dominated by fine grain sizes and this is attributed to phreatomagmatism. But could explosive magma–water interaction alone produce the strong hydration in this sample? Because phreatomagmatic fragmentation involves rapid quenching and only brief contact between high-temperature magma and external water substantial post-fragmentation hydration probably occurred. The dominant particle size of B120a is skewed towards the coarse grain sizes and thus fragmentation was probably driven by magmatic volatile exsolution. Here, weaker alteration or hydration could be due to its lower surface area-to-volume ratio, which would impede the ingress of water into the particles. D-0016 is dominated by fine grain sizes, indicating phreatomagmatic fragmentation, but the finer grain-size fraction is the most volatile rich, showing that pervasive alteration had not occurred. D-0016 contains more obsidian at the finer size fractions, compared with the coarser fractions and with D85a. Some of these obsidian particles appear perlitized under a petrological microscope. The perlitization could account for the volatile enrichment in the finer particles. Therefore the proportion of pristine obsidian a fragmental deposit contains as well as the degree of obsidian perlitization could be other factors controlling the total volatile content.

There is greater scatter between the endotherm, dTG and MS water signal peak temperature data at low volatile contents (Fig. 6). This is due to the way the volatiles (mostly water) coordinate with the host structure (Stolper 1982). The relative concentrations of water species under equilibrium state are dependent on temperature and total water concentration (H_2O_t) (Yokoyama *et al*. 2008). At low H_2O_t OH dominates over molecular water (H_2O_m) but the concentration of H_2O_m gradually increases relative to OH as H_2O_t increases (Stolper 1982). The scatter between the peak temperatures is greatest for obsidians (Fig. 6), as water accounts for a smaller proportion of the exsolved volatiles and most of the water is magmatic water. Jambon *et al*. (1992) reported dehydration temperatures of 510–980 °C for obsidians containing 0.114 wt% H_2O, indicating a large range over which magmatic water (which is an integral part of the tetrahedral structure) is exsolved. The three peak temperatures coincide slightly better for the perlites. Most of the additional water at these H_2O_t concentrations (2.5–8.15 wt%), assuming high-temperature hydration, will be bound as silanol groups (Si–OH) (Stolper 1982). The silanol groups are more weakly bound than magmatic water and so will break at lower temperatures. The hyaloclastites contain, in general, even more water, reflected in an even greater correspondence between the temperatures of the three peaks (Fig. 6). This is due to the increased dominance of weakly bound molecular water (Stolper 1982), which will exsolve at relatively low temperatures (Sodeyama *et al*. 1999; Roulia *et al*. 2006) controlled more by the boiling point of water than the activation energy required to break bonds.

The equation of a linear best-fit trend line drawn through the endotherm data (Fig. 6) is $T_E = -64.176V_T + 694.02$, with an R^2 value of 0.88, where T_E is the endotherm temperature and V_T the total volatile content. This indicates that a volatile-free glass would have an endotherm at 694 °C, which agrees well with degassing results for obsidian reported by Jambon *et al*. (1992) and T_g temperatures for Krafla obsidian (Castro *et al*. 2008). When volatile concentrations approach *c*. 9 wt% exsolution occurs at *c*. 100°C (Fig. 6). Sample heating at 110 °C was carried out during sample preparation to remove any surface water adsorbed during preparation. Such preparation could therefore result in some volatile loss from the most altered samples prior to TGA. The decreasing temperature of the endotherm of degassing as the total volatile content increases is, we believe, a function of increased alteration or hydration resulting in a greater proportion of H_2O_m (released at lower temperatures) relative to OH (Stolper 1982; Sodeyama *et al*. 1999; Roulia *et al*. 2006).

Table 5 shows that the green most volatile-rich samples have concentrations of mordenite and heulandite that are higher than or the same as those of the grey samples (with the exception of the perlitic samples, where the heulandite concentrations were constant within analytical error). The degassing temperature of the volatile-rich samples (100–200 °C, Fig. 6) is at the lower end of the estimate for the breakdown of heulandite (50–300 °C) and mordenite (70–6300 °C) (Cruciani 2006). Mordenite is formed preferentially over (and often from) heulandite (Kusakabe *et al*. 1981; Kitsopoulos 1997) at temperatures of 120–400 °C. Therefore the green samples must have been altered at temperatures between 120 and 400 °C, but a substantial amount of the alteration of B194a must have occurred below 120 °C as a result of the presence of heulandite (Kusakabe *et al*. 1981; Kitsopoulos 1997). The high total volatile content and greater proportion of relatively water-rich zeolite minerals of the green samples reflect the influence of hydrothermal activity on the samples. These samples could therefore represent a juvenile soil.

Zeolites are found in some andisols and are indicative of the

parent material containing hydrothermally formed material (Ping 2000). Mordenite is usually found with heulandite minerals in hydrothermal areas as an alteration product within volcaniclastic sequences (Kitsopoulos 1997). The strongly altered, zeolite-bearing volatile-rich samples of this study (B194a, B25a and D85a) may all represent juvenile andisols. Gennadiev *et al*. (2007) showed that the soil type present in the Torfajökull area is a vitrisol (a type of cryand; a common Icelandic andisol). Vitrisols contain $<1\%$ of organic carbon, support a 5–10% surface vegetation cover and contain $\geqslant 30\%$ of volcanic glass (Gennadiev *et al*. 2007). Thus, we believe that the volatile-rich green samples in this study represent juvenile soils and the grey perlites represent an intermediate stage in the alteration of pristine obsidians to soils.

Conclusion

(1) The total volatile content of rhyolitic obsidian increases with the degree of perlitization. The results from the perlites reveal that as the degree of perlitization increases the total volatile content increases, confirming that perlitization is driven by the ingress of external water.

(2) As the total volatile content increases the temperature of volatile exsolution decreases. The peak degassing temperatures reveal that as the volatile concentration increases the temperature of exsolution decreases. The scatter of the results reflects the way the inward diffusing volatiles (water) are bound to the host structure.

(3) A substantial volatile enrichment is often accompanied by secondary mineral growth. The green volatile-rich samples contain zeolite minerals (mordenite and heulandite), which add significant amounts of volatiles to the crystalline proportion of the samples but cannot account for the total volatile enrichment. The presence of zeolites suggests that these samples represent juvenile soils and that the grey perlites are an intermediary between volatile-free obsidian and soils.

The authors thank two anonymous reviewers and D. Pyle for comments that greatly improved the manuscript. H.T. was supported by an NERC Research Fellowship.

References

Bagdassarov, N., Ritter, F. & Yanev, Y. 1999. Kinetics of perlite glasses degassing: TG and DSC analysis. *Glass Science and Technology—Glastechnische Berichte*, **72**, 277–290.

Castro, J.M., Beck, P., Tuffen, H., Nichols, A. & Dingwell, D.B. 2008. Timescales of spherulite crystallization in obsidian inferred from water concentration profiles. *American Mineralogist*, **93**, 1816–1822.

Cruciani, G. 2006. Zeolites upon heating: Factors governing their thermal stability and structural changes. *Journal of Physics and Chemistry of Solids*, **67**, 1973–1994.

Davis, B.K. & McPhie, J. 1996. Spherulites, quench fractures and relict perlite in a Late Devonian rhyolite dyke, Queensland, Australia. *Journal of Volcanology and Geothermal Research*, **71**, 1–11.

Deer, W.A., Howie, R.A. & Zussman, J. 1963. *Rock-forming Minerals, Vol. 4: Framework Silicates*. Longman, Harlow.

Drysdale, D.J. 1991. Perlitic texture and other fracture patterns produced by hydration of glassy rocks. *Department of Geology, University of Queensland Papers*, **12**, 278–285.

Friedman, L. & Smith, R.L. 1958. The deuterium content of water in some volcanic glasses. *Geochimica et Cosmochimica Acta*, **15**, 218–228.

Friedman, I. & Smith, R.L. 1960. A new dating method using obsidian: Part 1, the development of the method. *American Antiquity*, **25**, 476–522.

Friedman, I., Smith, R.L. & Long, W.D. 1966. Hydration of natural glass and formation of perlite. *Geological Society of America Bulletin*, **77**, 323–328.

Gennadiev, A.N., Geptner, A.R., Zhidkin, A.P., Chernyanskii, S.S. & Pikovskii, Yu. I. 2007. Exothermic and endothermic soils of Iceland. *Eurasian Soil Science*, **40**, 595–607.

Gunnarsson, B., Marsh, B.D. & Taylor, H.P., Jr 1998. Generation of Icelandic rhyolites: silicic lavas from the Torfajökull central volcano. *Journal of Volcanology and Geothermal Research*, **83**, 1–45.

Heiken, G. 1972. Morphology and petrography of volcanic ashes. *Geological Society of America Bulletin*, **83**, 1961–1987.

Heiken, G. & Wohletz, K. 1985. *Volcanic Ash*. University of California Press, Berkeley 18.

Jambon, A., Zhang, Y.X. & Stolper, E.M. 1992. Experimental dehydration of natural obsidian and estimation of dH_2O at low water contents. *Geochimica et Cosmochimica Acta*, **56**, 2931–2935.

Jónasson, K. 2007. Silicic volcanism in Iceland: Composition and distribution within the active volcanic zones. *Journal of Geodynamics*, **43**, 101–117.

Kitsopoulos, K.P. 1997. The genesis of a mordenite deposit by hydrothermal alteration of pyroclastics on Polyegos Island, Greece. *Clay and Clay Minerals*, **45**, 632–648.

Kusakabe, H., Minato, H., Utada, M. & Yamanaka, T. 1981. Phase relations of clinoptilolite, mordenite, analcime, and albite with increasing pH, sodium ion concentration, and temperature. *University of Tokyo Scientific Papers, College of General Education*, **31**, 39–59.

Marshall, R.R. 1961. Devitrification of natural glass. *Geological Society of America Bulletin*, **72**, 1493–1520.

Mathews, W.H. 1947. 'Tuyas,' flat-topped volcanoes in northern British Columbia. *American Journal of Science*, **245**, 560–570.

McGarvie, D.W. 1984. Torfajökull: a volcano dominated by magma mixing. *Geology*, **12**, 685–688.

McPhie, J., Doyle, M. & Allen, R. 1993. *Volcanic Textures. A guide to the interpretation of textures in volcanic rocks*. Centre for Ore Deposit and Exploration Studies, University of Tasmania, Hobart.

Newman, S., Stolper, E.M. & Epstein, S. 1986. Measurement of water in rhyolitic glasses: calibration of an infrared spectroscopic technique. *American Mineralogist*, **71**, 1527–1541.

Noh, J.H. & Boles, J.R. 1989. Diagenetic alteration of perlite in the Guryongpo area, Republic of Korea. *Clays and Clay Minerals*, **37**, 47–58.

Ping, C.-I. 2000. Volcanic soils. *In:* Sigurdsson, H., Houghton, B.F., McNutt, S.R., Rymer, H. & Stix, J (eds) *Encyclopedia of Volcanoes*. Academic Press, London, 1259–1270.

Ross, C.S. & Smith, R.L. 1955. Water and other volatiles in volcanic glasses. *American Mineralogist*, **40**, 1071–1089.

Roulia, M., Chassapis, K., Kapoutsis, J.A., Kamitsos, E.I. & Savvidis, T. 2006. Influence of thermal treatment on the water release and the glassy structure of perlite. *Journal of Material Science*, **41**, 5870–5881.

Saisuttichai, D. & Manning, D.A.C. 2007. Geochemical characteristics and expansion properties of a highly potassic perlitic rhyolite from Lopburi, Thailand. *Resource Geology*, **57**, 301–312.

Sæmundsson, K. 1978. Fissure swarms and central volcanoes of the neovolcanic zones of Iceland. *Geological Journal, Special Issue*, **10**, 415–432.

Sodeyama, K., Sakka, Y. & Kamino, Y. 1999. Preparation of fine expanded perlite. *Journal of Material Science*, **34**, 2461–2468.

Stolper, E.M. 1982. Water in silicate glasses: An infrared spectroscopic study. *Contributions to Mineralogy and Petrology*, **81**, 1–17.

Tuffen, H. 2001. *Subglacial rhyolite volcanism at Torfajökull, Iceland*. PhD thesis, Open University, Milton Keynes.

Tuffen, H. & Castro, J. 2009. The emplacement of an obsidian dyke through thin ice: Hrafntinnuhryggur, Krafla Iceland. *Journal of Volcanology and Geothermal Research*, doi:10.1016/j.jvolgeores.2008.10.021.

Tuffen, H., Gilbert, J. & McGarvie, D. 2001. Products of an effusive subglacial rhyolite eruption: Bláhnúkur, Torfajökull, Iceland. *Bulletin of Volcanology*, **63**, 179–190.

Tuffen, H., McGarvie, D.W., Gilbert, J.S. & Pinkerton, H. 2002. Physical volcanology of a subglacial-to-emergent rhyolitic tuya at Rauðufossafjöll, Torfajökull, Iceland. *In:* Smellie, J.L. & Chapman, M.G. (eds) *Volcano–Ice Interaction on Earth and Mars*. Geological Society, London, Special Publications, **202**, 213–236.

Tuffen, H., McGarvie, D.W., Pinkerton, H., Gilbert, J.S. & Brooker, R.A. 2008. An explosive–intrusive subglacial rhyolite eruption at Dalakvísl, Torfajökull, Iceland. *Bulletin of Volcanology*, **70**, 841–860.

Walker, G.P.L. 1963. The Breiddalur central volcano, eastern Iceland. *Quarterly Journal of the Geological Society of London*, **119**, 29–63.

Yokoyama, T., Okumura, S. & Nakashima, S. 2008. Hydration of rhyolitic glass during weathering as characterized by IR microspectroscopy. *Geochimica et Cosmochimica Acta*, **72**, 117–125.

Received 14 January 2009; revised typescript accepted 20 March 2009.
Scientific editing by David Pyle.